Journal of the European Ceramic Society 21 (2001) 2811–2819
www.elsevier.com/locate/jeurceramsoc

Microstructure and properties of various fluorine-containing SiAlON ceramics synthesized by HIPing

S. Shimada [a],*, M. Tanaka [a], H. Kiyono [a], K.J.D. MacKenzie [b]

[a] Graduate School of Engineering, Hokkaido University, Sapporo 060-8682, Japan
[b] New Zealand Institute for Industrial Research and Development, PO Box 31-310, Lower Hutt, New Zealand

Received 30 November 2000; received in revised form 6 February 2001; accepted 17 February 2001

Abstract

An attempt was made to prepare various F-doped β-, O-, X-, and α-SiAlONs from a mixture of Si_3N_4, SiO_2, Al_2O_3, AlN, or Y_2O_3 using AlF_3 or topaz as the fluorine source by HIPing at 1500–1800°C and 150 MPa. The phases were identified and the z, x, and m/n values determined for β-, O-, and α-SiAlONs by X-ray diffraction. When AlF_3 was used, a single phase ceramic (O-SiAlON) was produced from a mixture of α-Si_3N_4 and SiO_2 at 1500°C, with a mixture of O- and β-SiAlONs formed at 1700°C. A mixture of α-Si_3N_4, AlN, and Y_2O_3 with AlF_3 produced β-/Y-α-SiAlON ceramics at 1730°C. The use of topaz produced the β-SiAlON ceramic with a trace of mullite from a mixture of α-Si_3N_4 and AlN at 1770°C and mixed phase β-/O-SiAlON ceramics from α-Si_3N_4 and SiO_2 at 1700°C. Single phase X-SiAlON could not be obtained under the present conditions. The microstructures of the single phase O- and β-SiAlON ceramics and the β-/Y-α-SiAlON mixture showed the growth of O- and β-SiAlON and Y-α-SiAlON crystals with hexagonal and/or long rod-like or platy shapes in a matrix of F-containing glassy phase. The compositions of the SiAlON crystals and the glass phase were semi-quantitatively determined by EDX; the total glass phase was estimated by a quantitative Rietveld XRD powder method. The F-doped β-SiAlON ceramics showed better corrosion resistance towards NaCl vapor and lower Vickers hardnesses. © 2001 Elsevier Science Ltd. All rights reserved.

Keywords: Corrosion; Fluorine; Hot isostatic pressing; Microstructure-final; SiAlONs

---

1. Introduction

SiAlONs are compounds containing silicon, aluminum, oxygen and nitrogen which have found applications as engineering ceramics, cutting tools, and abrasive materials.[1] They occur with various compositions and structures, of which the most thoroughly studied are α-, β-, O- and X-SiAlON and mixtures of these phases.[1,2] β-SiAlON is structurally related to β-Si_3N_4 and has the composition, $Si_{6-z}Al_zO_zN_{8-z}$, where z ranges from 0, corresponding to pure Si_3N_4, to ca. 4.3. O-SiAlON may be regarded as Al-substituted silicon oxynitride, with the composition, $Si_{2-x}Al_xO_{1+x}N_{2-x}$, where x ranges from 0 (pure Si_2N_2O) to ca. 0.4 at 1900°C. X-SiAlON ($Si_{12}Al_{18}O_{39}N_8$) has a structure similar to mullite ($Al_6Si_2O_{13}$) and exists over a narrow solid solution range between Si_3N_4 and mullite. α-SiAlON can be written in terms of the general formula $Me_mSi_{12-(pm+n)}Al_{(pm+n)}O_nN_{16-n}$ and contains metal ions Me^{p+}.

There is an interest in the densification of such SiAlON ceramics and the measurement of their mechanical properties.[3,4] For SiAlONs to achieve full density, small amounts of various metal oxides such as MgO, CaO, Y_2O_3 are added to aid sintering under pressureless or pressurized conditions.[5–7] These added metal oxides react with the SiO_2 present on the Si_3N_4 surfaces, resulting in the formation of amorphous and/or crystalline secondary phases at grain boundaries and/or multi-grain junctions. The mechanical properties and the oxidation or corrosion behavior of SiAlONs at high temperatures strongly depend on the volume fraction and composition of grain boundary crystalline or amorphous phases.[8–12] It is thus important to control the grain boundary composition and structure to improve the mechanical and corrosion-resistance properties.

Hot pressing (HP) or hot isostatic pressing (HIP) is well known as techniques which can be used to densify SiAlON ceramics. HIPing is recognized as a particularly

---

* Corresponding author. Fax: +81-11-706-6576.
E-mail address: shimashi@eng.hokudai.ac.jp (S. Shimada).

PII: S0955-2219(01)00216-3

useful method for attaining fully densified SiAlON ceramics. Ekstrom et al. have used this technique to densify many silicon nitride-related ceramics both with and without small amounts of additives.[13] For example, dense β-silicon nitride ceramics were prepared by HIPing at 1750°C with small amounts of Al_2O_3 and AlN. The HIPing method has an advantage over HP in that pressure is transmitted isostatically to the whole sample using a glass-encapsulated ampoule, constituting a completely enclosed system in which volatile materials are retained.

Several studies have been reported on the use of fluorine in silicon nitride system to control the composition, oxidation, and optical properfies.[14–16] Jun et al. have produced amorphous fluorinated Si_3N_4 films using a mixture of SiH_4, N_2 and NF_3 gases by an inductively coupled plasma enhanced CVD method.[14] Kleebe et al. reported the formation and mechanical properties of fluorine-doped Si_3N_4–SiC ceramics, using polytetrafluoroethylene (Teflon) as the source of fluorine and observed segregation of fluorine at grain and phase boundaries, leading to a decrease in the cohesive interface strength.[15,16] If SiAlONs can be fluorinated, there is a possibility of F ions to be incorporated in the SiAlON and grain boundary structures, with possible changes in the structure and composition, which could lead to changes in the mechanical and oxidation/corrosion properties. In particular, the latter property should be improved, because fluorine is not readily replaced by gases such as oxygen or chlorine due to its higher electro-negativity. However, the synthesis of fluorinated SiAlONs has not been reported. A primary consideration in the preparation of F-doped SiAlON is the compound to be used as the F-source. AlF_3 and topaz should be suitable sources of fluorine for this purpose, because they also contain the Al and/or Si constituents of the SiAlON.

This work investigates the effect of both AlF_3 or topaz as sources of fluorine and their influence on the formation and densification of β-, O-, X-, and α-SiAlONs prepared by HIPing. The sample for HIPing is encapsulated in glass, preventing the loss of fluorine from the closed reaction system. The microstructures of the F-doped SiAlONs composites were examined to determine the location of the fluorine in the SiAlON ceramics. The corrosion resistance of F-doped β-SiAlON towards NaCl vapor and their Vickers hardnesses were compared with those of F-free β-SiAlON ceramics.

2. Experimental

The starting powders used for synthesis of β-, O- and X-SiAlON were α-Si_3N_4, SiO_2, γ-Al_2O_3, and AlN. For synthesis of Y-α-SiAlON, Y_2O_3 powder was added to the above mixtures. AlF_3 and topaz powders were used as the source of fluorine. Topaz ($Al_2SiO_4(F,OH)_2$) contains alumina and silica which are incorporated as a constituent of SiAlON. CaF_2 was also used as a source of fluorine in an attempted synthesis of F-doped Ca-α-Siaon. Table 1 summarizes the details and nominal compositions of the starting mixtures used in three experiments. The reactants were thoroughly mixed in a mortar and dried at 100°C. Pellets 12 mm diameter × 5 mm height were made from the mixed powders by cold isostatic pressing at 400 MPa, embedded in fine BN powder, and encapsulated by sealing in a glass tube. The pellet was sintered by HIPing under N_2 gas pressure of 150 MPa in the temperature range 1500–1800°C for 2 h. After HIPing, the pellet was powdered for the phase identification by X-ray diffraction (XRD). The lattice parameters (a_o and c_o) of the α-, β-, and O-SiAlON compositions were measured by XRD using Si powder as the internal standard. The z value in $Si_{6-z}Al_zO_zN_{8-z}$ was calculated using the linear relationship between the z-values and the lattice parameters.[13]

$$a_o\ (A) = 7.6036 + 0.02964z$$

$$c_o\ (A) = 2.9078 + 0.02556z$$

For O-SiAlON ($Si_{2-x}Al_xO_{1+x}N_{2-x}$), the following equation was used,[17] to determine the compositional parameter (x) from the measured b_o value:

$$b_o\ (A) = 8.878 + 0.156x$$

The composition of Y-α-SiAlON can be written in the general formula $Y_xSi_{12(m+n)}Al_{(m+n)}O_nN_{16-n}$ for a metal ion Y^{3+}.[18]

$$a_o\ (A) = 7.752 + 0.036m + 0.02n$$

$$c_o(A) = 5.620 + 0.031m + 0.04n$$

The hardness measurements (H) were performed using a Vickers diamond pyramidal indenter with a load of 300 g, taking the average of five indentations.

The surfaces of the densified SiAlON ceramics were polished with 3 μm diamond paste and their back-scattering electron images observed using an SEM (BEI-SEM). The distribution of SiAlON and F in the surface was determined by wave-length-dispersive (WDX) X-ray microanalysis (XMA). Thin foils of the HIPed samples were prepared by mechanical dimple-thinning and repeated ion milling. The microstructures of the samples were examined using transmission electron microscope operating at 300 kV. Chemical analyse for SiAlON, F, Ca or Y in the single phase β-, O- and Ca- or Y-α-SiAlONs were performed on the thin foil samples by EDX. The volume fraction of glassy phase in the single phase

Table 1
Composition of the starting mixtures and identification of product obtained by HIPing

Run No.	Composition (mol)						Temp. (°C)	Nominal phase composition		Identification of products
	α-Si_3N_4	SiO_2	Al_2O_3	AlN	AlF_3					
1	1.0		1.0		1.0		1500	β	$Si_3Al_3O_3N_4F_3$	β-SiAlON > AlF_3, unknown, Al_2O_3 $\gg$ α-Si_3N_4
2	1.0		1.0		1.0		1700	β	$Si_3Al_3O_3N_4F_3$	β-SiAlON ($z=1.8$) > mullite, unknown, AlF_3
3	2/3	1.0	1/2	1.0	1.0		1500	β	$Si_3Al_3O_{3.5}N_{3.7}F_3$	β-SiAlON ($z=1.0$) > unknown, α-Si_3N_4, Al_2O_3
4	2/3	1.0	1/2	1.0	1.0		1700	β	$Si_3Al_3O_{3.5}N_{3.7}F_3$	β-SiAlON ($z=1.0$) > mullite, unknown, AlF_3, Al_2O_3
5	1.0[a]				1.0		1700	β	$Si_3A_{13}O_{2.1}N_{4.7}F_{2.5}$	β-SiAlON ($z=1.8$) > AlF_3, 15R-SiAlON, mullite,Al_3O_3N
6	10.0[a]				1.0		1700	β	$Si_{2.95}Al_{3.05}O_{2.95}N_{4.92}F_{0.3}$	β-SiAlON ($z=2.6$) ~ X-SiAlON
7	1/3	1/5			4/5		1500	O	$Si_{1.8}Al_{0.2}O_{1.6}N_{1.3}F_{0.6}$	O-SiAlON ($x=0.1$)
8	1/3	1/5			4/5		1700	O	$Si_{1.8}Al_{0.2}O_{1.6}N_{1.3}F_{0.6}$	0-SiAlON ($x=0.06$) > β-SiAlON
9	1.0	3.0	4.0		1.0		1500	X	$Si_{12}Al_{18}O_{36}N_8F_6$	mullite > β-Si_3N_4, AlF_3
10	1.0	3.0	4.0	1/2	1/2		1500	X	$Si_{12}Al_{18}O_{36}N_9F_3$	X-SiAlON > β-Si_3N_4
11	1.0	3.0	4.0	1/2	1/2		1700	X	$Si_{12}Al_{18}O_{36}N_9F_3$	mullite ~ β-Si_3N_4 > AlF_3, X-SiAlON
	α-Si_3N_4	SiO_2	Al_2O_3	AlN		topaz				
12	1.0			2.0		1.0	1700	β	$Si_3Al_3O_3N_{4.5}F_{1.5}$	β-SiAlON ($z=2.3$)$\gg$ mullite
13	1.0			2.0		1.0	1770	β	$Si_3Al_3O_3N_{4.5}F_{1.5}$	β-SiAlON ($z=0.4$) $\gg$ > mullite
14	5.0	2.0				1.0	1700	O	$Si_{1.8}Al_{0.2}O_{0.8}N_2F_{0.2}$	O-SiAlON ($x=0.12$) ~ β-SiAlON ($z=0.6$)
15	5.0	2.0				1.0	1800	O	$Si_{1.8}Al_{0.2}O_{0.8}N_2F_{0.2}$	β-SiAlON ($z=1.8$)$\gg$ mullite ~ AlF_3
16	1.0	2.0		4.0		7.0.	1700	X	$Si_{12}Al_{18}O_{32}N_8F_{14}$	mullite ~ AlF_3 > β-Si_3N_4
	α-Si_3N_4	Y_2O_3	Al_2O_3	AlN	AlF_3	CaF_2				
17	13.0		2.0	7.0		3.0	1700	α	$Ca_{0.72}(Si_{9.36}Al_{2.64})$ $(O_{1.44}N_{14.16}j6F_{1.44})$	β-Si_3N_4 > CaF_2
18	13.0	1.0			9.0		1760	α	$Y_{0.5}(Si_{9.75}Al_{2.25})$ $(O_{0.75}N_{13}F_{6.75})$	β-Si_3N_4 $\gg$ AlF_3, unknown
19	13.0	1.0		6.0	3.0		1780	α	$Y_{0.5}(Si_{9.75}Al_{2.25})$ $(O_{0.75N}N_{14.5}F_{2.25}$	β-Si_3N_4 $\gg$ Y-α-SiAlON, unknown
20	13.0	1.0		8.0	1.0		1730	α	$Y_{0.5}(Si_{9.75}Al_{2.25})$ $(O_{0.75}N_{15}F_{0.75})$	β-SiAlON ($z=0.3$) Y-α-SiAlON $\gg$ unknown

[a] β-SiAlON ($z=3$) was used.

F-containing β-SiAlON ceramic was quantitatively determined using a Rietvelt-based XRD procedure (SIROQUANT).

The corrosion of single phase F-containing β-SiAlON ceramic was studied at 1300°C for 3 h in flowing N_2 gas (50 ml min^{-1}) containing a constant concentration of NaCl vapor (1.0 g h^{-1}), generated by heating powdered NaCl at about 860°C. For comparison, a pure β-SiAlON ceramic with a similar z value prepared by HIPing was corroded under the same conditions. The corroded ceramics were embedded in epoxy resin, sectioned and polished. The corroded scale was observed in cross-section by SEM and elemental maps of SiAlON and F in the scale were obtained by WDX-XMA.

3. Results and discussion

3.1. Phase identification

The phases present in the products obtained by HIPing the various starting mixtures at 1500–1800°C are summarized in Table 1. F-containing β-SiAlON ceramics were obtained from a mixture of α-Si_3N_4, Al_2O_3 and AlF_3 (Runs 1 and 2). The products of Run 1 include β-SiAlON as the major phase with small amounts of unreacted AlF_3 and Al_2O_3 and a trace of α-Si_3N_4. At 1700°C, the amount of β-SiAlON ($z=1.8$) increases at the expense of α-Si_3N_4 and Al_2O_3, but an undesired mullite phase is also formed with unreacted AlF_3 (Run 2). A mixture of SiO_2, AlN, α-Si_3N_4 and Al_2O_3 in the presence of AlF_3 was reacted at 1500 and 1700°C (Runs 3 and 4). At 1500°C, β-SiAlON ($z=1.0$) is the major product, but α-Si_3N_4 and Al_2O_3 are still present. Increasing the temperature to 1700°C produces β-SiAlON ($z = 1.0$) as the major phase with small amounts of mullite and unreacted AlF_3 and Al_2O_3 (Run 4). At the higher temperature of 1700°C (Runs 2 and 4), mullite is formed prior to the formation of β-SiAlON. Direct reaction of β-SiAlON ($z=3.0$) with equimolar AlF_3 at 1700°C gives β-SiAlON with a decreased z value (1.8), together with minor phases of l5R-SiAlON, mullite, Al_3O_3N and a small amount of unreacted AlF_3 (Run 5). In another mixture of β-SiAlON with AlF_3 in a 10 fold molar ratio of β-SiAlON, mixed phases of β-SiAlON ($z=2.6$) and X-SiAlON were formed and the AlF_3 was fully consumed

(Run 6). In both cases, the z value was reduced from 3.0 to 1.8 or 2.6.

O-SiAlON was synthesized by HIPing α-Si_3N_4 with SiO_2 in the presence of AlF_3 at 1500 and 1700°C (Runs 7 and 8). Single phase O-SiAlON with $x = 0.1$, close to the expected x value (0.2) was formed at 1500°C. The XRD pattern of the O-SiAlON is shown in Fig. 1(a). A small unidentified peak (marked x) is observed. At 1700°C. mixtures of O- and β-SiAlONs were produced (Run 8), as shown by XRD [Fig. 1(b)].

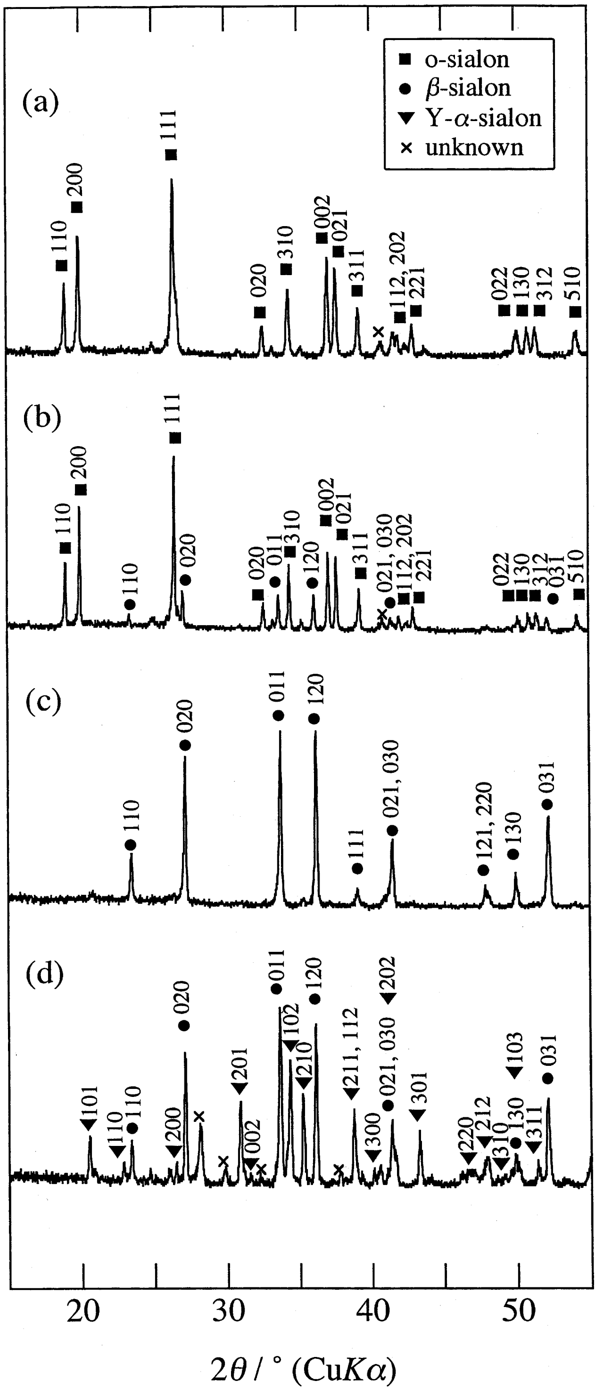

Fig. 1. X-ray diffraction patterns of various F-containing SiAlON ceramics. (a) O-SiAlON, (b) mixed O-/β-SiAlONs, (c) β-SiAlON, (d) mixed β-/Y-α-SiAlONs.

For synthesis of X-SiAlON (Runs 9–11), a mixture of α-Si_3N_4, SiO_2 and Al_2O_3 with and without AlN was reacted in the presence of AlF_3 at 1500 and 1700°C. X-SiAlON was not produced in the absence of AlN, but mullite was formed with the concomitant transformation of α- to β-Si_3N_4 (Run 9). The addition of 0.5 mol AlN produces X-SiAlON and β-Si_3N_4 at 1500°C (Run 10), but the higher temperature of 1700°C favors the formation of mullite (Run 11). The results of Runs 9–11 indicate that mullite is more readily formed in preference to X-SiAlON. The preferential formation of mullite consumes SiO_2 and Al_2O_3 in the mixture, shifting it away from the appropriate formation region of X-SiAlON.

In Runs 1–11, AlF_3 was used as the source of fluorine. Except for Runs 7 and 8 where single phase O-SiAlON and a mixture of O- and β-SiAlONs were produced, unreacted AlF_3 always remained in the sample, possibly due to its low reactivity. A more reactive fluorine source was, therefore, sought for the formation of F-containing SiAlON ceramics of the desired composition. It is well known that the thermal decomposition of oxy-salts, clays, or minerals can produce reactive compounds. Topaz ($Al_2SiO_4(F,OH)_2$) is potentially such a fluorinating agent, since it thermally decomposes to mullite,[20] releasing a reactive fluorine compound and H_2O, which could be incorporated into the encapsulating glass. An additional advantage of using topaz is that the aluminosilicate decomposition product can become part of the desired SiAlON. A mixture of α-Si_3N_4, AlN and topaz in the mol ratio 1:2:1, corresponding to a nominal β-SiAlON composition of $Si_3Al_3O_3N_{4.5}F_{1.5}$, was reacted at 1700°C (Run 12). The product was β-SiAlON ($z = 2.3$) with a very small amount of mullite. A higher temperature experiment at 1770°C (Run 13) resulted in the formation of β-SiAlON ($z = 0.4$) with a trace of mullite. The XRD pattern of this phase β-SiAlON is shown in Fig. 1(c).

A mixture of α-Si_3N_4 and SiO_2 containing topaz with the nominal composition of O-SiAlON was reacted at 1700 and 1800°C (Runs 14 and 15). At 1700°C, a mixture of O-SiAlON with $x = 0.12$ and β-SiAlON with $z = 0.6$ was produced, with an XRD pattern similar to Fig. 1(b). The product at 1800°C was β-SiAlON ($z = 1.8$) with a very small amount of mullite and unreacted AlF_3. An attempt to produce X-SiAlON from a mixture containing topaz was unsuccessful, giving mullite, unreacted AlF_3 and β-Si_3N_4 (Run 16).

The synthesis of F-doped α-SiAlON was attempted using AlF_3 or CaF_2 as the source of fluorine. Ca-α-SiAlON was sought using a mixture of CaF_2, α-Si_3N_4, Al_2O_3 and AlN (Run 17). The product of this run was β-Si_3N_4 and CaF_2 with no change in the X-ray intensity, suggesting that CaF_2 is stable for reaction in this mixture at a temperature of 1700°C in a closed system at 150

MPa. An attempt to produce single phase F-doped Y-α-SiAlON using higher molar ratios of AlF_3 (9.0 and 3.0) was unsuccessful, producing mainly β-Si_3N_4 (Runs 18 and 19). At a lower AlF_3 ratio (1.0), mixtures of β- and Y-α-SiAlONs were formed (Runs 20). Fig. 1(d) shows the XRD pattern of these mixed β-/Y-α-SiAlONs. Unidentified peaks were observed at almost the same 2θ positions in Runs 1–4 and 18–20.

3.2. Microstructure of F-doped SiAlONs

Microstructural observation and chemical analyses of the single phase O- and β-SiAlONs ceramics and the mixed O-/β- and Y-α-/β-SiAlONs ceramics were performed using BEI-SEM/TEM and WDX-XMA, respectively. Fig. 2 (A) shows a BEI-SEM image of sintered surface of the single phase O-SiAlON ceramic, which contains randomly oriented needle- and rod-like crystals 1–5 μm long and 0.5–1 μm wide. The TEM image [Fig. 2(B)] reveals the growth of long rod-like crystals 0.2–0.5 μm wide with a high aspect ratio of about 30 together with 1.5 μm platy crystals in a glassy matrix. Table 2 shows the semi-quantitative elemental analysis of the single phases O- and β-SiAlONs, the mixed β-/Y-α-SiAlONs and the volume fraction of glassy phase estimated by TEM-EDX analysis. The O-SiAlON crystals contain Si, Al, O, and N with average atomic percentages of 32,2,27 and 40, respectively, but no F. The values of 2

Table 2
Semi-quantitative analysis of SiAlON crystals and glassy phase

Run	SiAlON		Element (at.%)						Volume fraction of glassy phase
			Si	Al	O	N	Y	F	
7	O-SiAlON	Crystals	32	2	27	40	–	–	
		Glassy phase	20	3	61	0	–	16	> 30%
13	β-SiAlON	Crystals	28	2	3	67	–	–	
		Glassy phase	19	2	57	13	–	9	> 20%
20	Y-α-SiAlON	Y-α-SiAlON crystals	32	6	3	58	2		
		β-SiAlON crystals	28	3	3	65	0		< 10%[a]

[a] Glassy phase contained 25 at.% F.

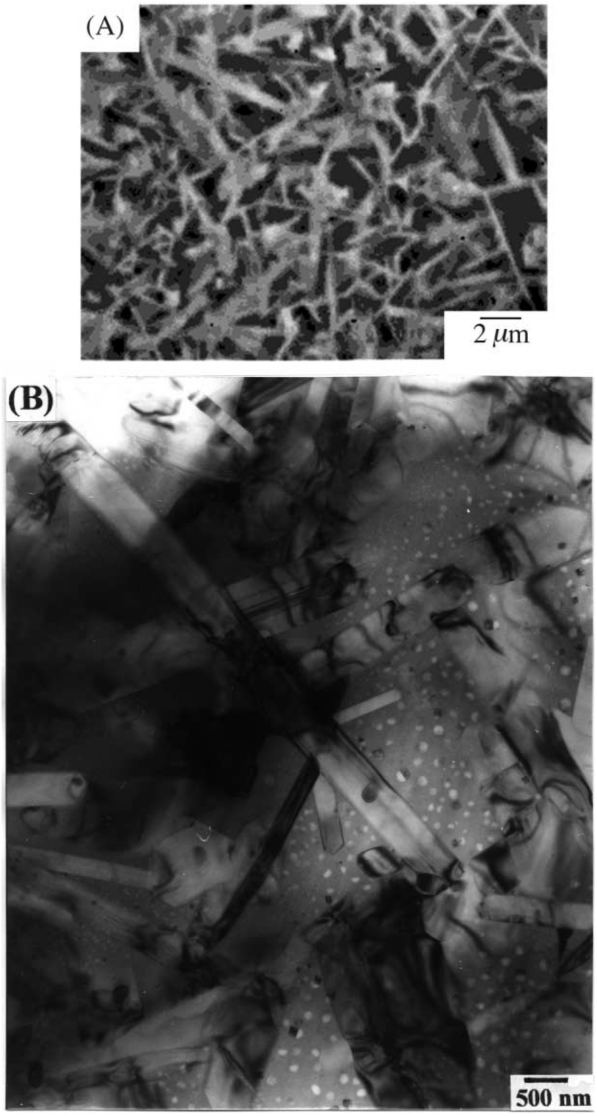

Fig. 2. BEI-SEM (A) and TEM (B) images of O-SiAlON ceramic.

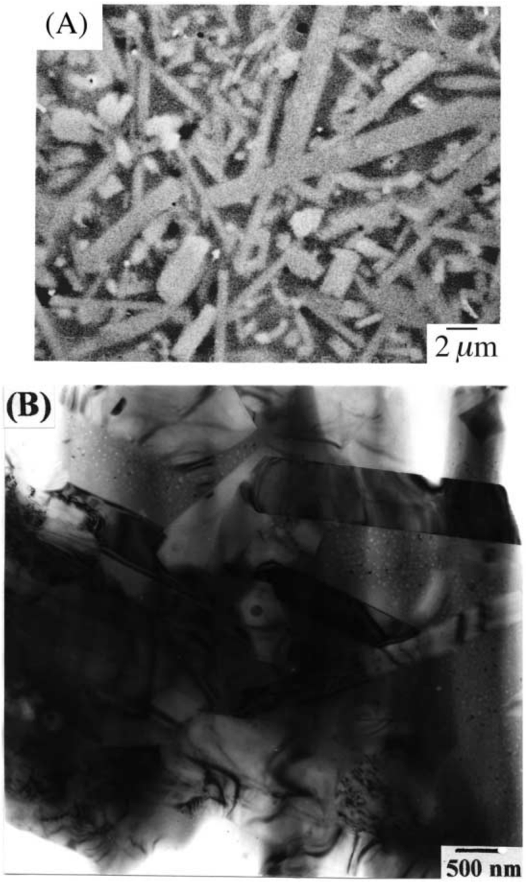

Fig. 3. BEI-SEM (A) and TEM (B) images of mixed O-/β-SiAlON ceramic.

at.% Al and 27 at.% O determined for the O-SiAlON crystals correspond to $x=0.1$, in good agreement with that calculated from XRD. The electron diffraction (ED) of the matrix showed a diffuse ring, consistent with a glassy phase, which contains Si, Al, O and F at concentration of 20, 3, 61 and 16 at.%, respectively, but no N (Table 2). The volume fraction of the glassy phase exceeds 30 vol.%, assisting the growth of the elongated O-SiAlON crystals with high aspect ratio. The numerous white spots observed in the glassy phase are probably pores. Higher temperatures (1700°C) caused the crystals to become long and relatively thick (Run 8), and increased their number, as shown in Fig. 3(A). The TEM image reveals the existence of a glassy phase, in which platy- or needle-like crystals have grown [Fig. 3(B)]. It was not possible to determine whether these crystals are O- or β-SiAlON.

Fig. 4(A) shows the BEI-SEM image of the β-SiAlON with a trace of mullite produced from a mixture of α-Si_3N_4, SiO_2, AlN and topaz (Run 13). Rod-like or platy crystals 1–3 μm wide and 2–5 μm long and hexagonal crystals 1–2 μm wide are seen. The existence of fluorine in the product was long and hexagonal crystals 1–2 μm wide are seen. The existence of fluorine in the product was confirmed by the elemental F map but it was not possible to determine the location of F by SEM-EDX. The TEM image of the single phase β-SiAlON is shown in Fig. 4(B). Hexagonal and rod-like crystals 0.5–1 μm wide with an aspect ratio less than 10 are seen to have grown in the matrix. As determined by EDX analysis (Table 2), the crystals are of an average composition, 28 at.% Si, 2 at.% Al, 3 at.% O and 67 at.% N, but do not contain F. The crystal shape and composition indicate that the hexagonal crystals are F-free β-SiAlONs. The Al and O content of the crystals is about 2 and 3at.%, corresponding to a z value of 0.4, in good agreement with that calculated from the XRD lattice measurement [Fig. 1(c)]. ED of the matrix showed a diffuse ring, indicative of a glassy phase, with the composition of 19 at.% Si, 2 at.% Al, 57 at.% O, 13 at.% N and 9 at.%F. An estimate of the crystal and glassy phase volumes from the TEM image indicates a glassy phase content greater than 20 vol.%. The fluorine content in the glassy phase is concentrated to about 9 at.% from the initial composition of 5 at.%. The chemical composition of the glassy phase suggests that it is a silicon oxynitride glass containing F.

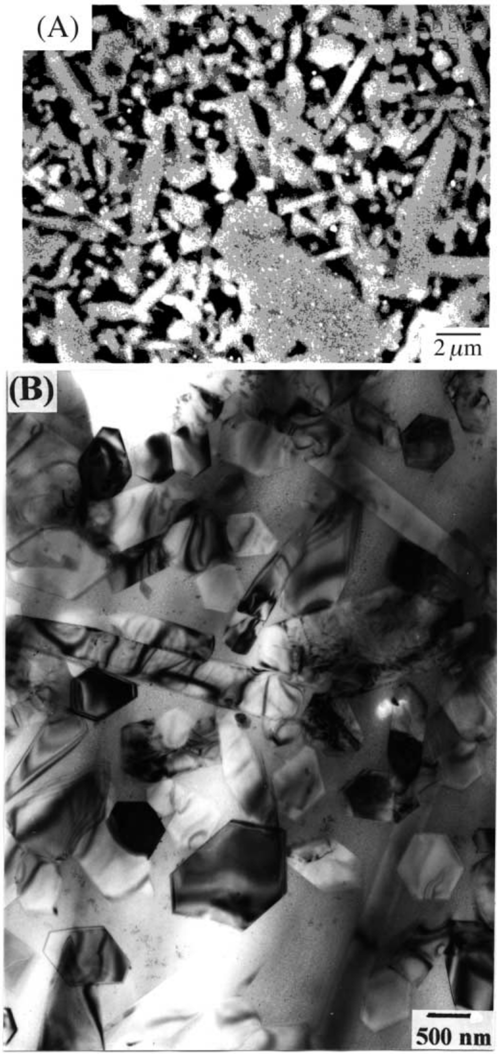

Fig. 4. BEI-SEM (A) and TEM (B) images of β-SiAlON ceramic.

Mixed Y-α-/β-SiAlONs were produced from a mixture of α-Si_3N_4, Y_2O_3, AlN and AlF_3 in a molar ratio of 13:1:8:1 (Run 20). The BEI-SEM image of the polished ceramic surface shows relatively dense microstructure containing gray and smaller white contrasting grains of β-SiAlON and α-SiAlON, respectively [Fig. 5(A)]. Elemental F was found by EDX to be distributed uniformly over the polished surface. The TEM image of a mixed SiAlON ceramic [Fig. 5(B)] indicates the development of either equiaxed or hexagonal grains containing no F in a glassy matrix. Since the equiaxed crystals contain 2 at.% Y, they may be identified as Y-α-SiAlON of the composition of $x=0.25$, in agreement with that calculated from the lattice measurement. The hexagonal crystals which contain no Y are identified as β-SiAlONs with $z=0.3$ consistent with the composition calculated from the lattice measurement The volume fraction of the glassy phase was less than 10 vol.% (Table 2), considerably less than in the ceramics containing single phases β- and O-SiAlONs. Some areas in the TEM image contain almost no glass, a characteristic of the microstructure of β-/Y-α-SiAlON ceramics. The F content in the glassy phase at the triple points between the grains can be as high as 25 at.%. It is concluded that the F is not incorporated into the SiAlON structure, but into the glassy phase, irrespective of the SiAlON type. The volume fraction of glass ranges from 10 to 30 vol.%. It is assumed that the presence of the glassy phase encourages the development of elongated β- or O-SiAlON grains with a high aspect ratio.

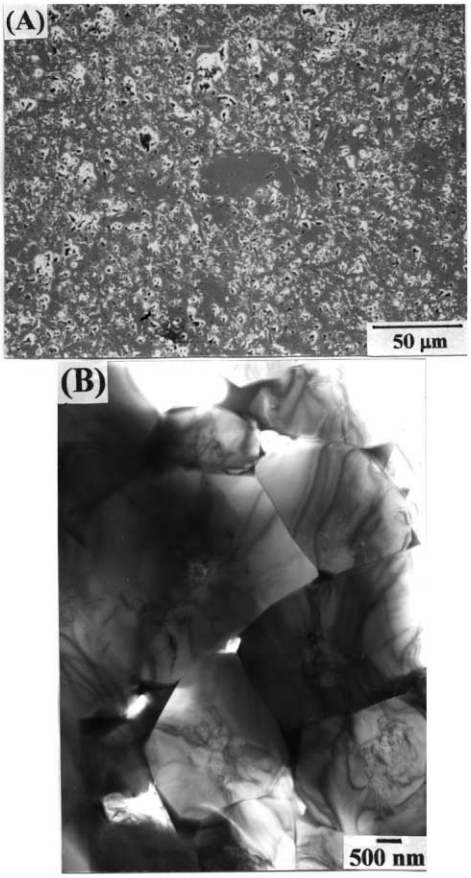

Fig. 5. BEI-SEM (A) and TEM (B) images of β-/Y-α-SiAlON ceramic.

3.3. *Constitution of the glassy phase in the sample of nominal β-SiAlON composition*

The total glass phase in the sample of β-SiAlON composition (Run 13) was estimated by a quantitative Rietveld XRD powder method[21] to be 35 mass%. Using this value as the basis for proportioning their EDX analytical results for the combined crystalline and glassy phase of Run 13 (Table 2) results in an estimate for the atomic composition of the glass of $Si_{6.7}Al_{0.7}O_{20}N_{4.6}F_3$. An alternative estimate of the glass composition was made from measurements of the amounts of the individual crystalline phases present (also obtained from the Rietveld analysis) together with a global analysis of the whole powder sample made by EPMA on five areas of 20×20 µm size. The Rietveld analysis indicated a whole-body composition of 56.4 mass% β-SiAlON of very low *z*-value, 4.7 mass% mullite, 35 mass% glass and 3.9 mass% Si (added as an internal standard for the cell parameter measurements). If the calculation is simplified by ignoring the Al content of the β-SiAlON, assuming the total F content resides in the glass and utilizing the ratio of Si in the crystalline phases to Si in the glass (Table 2), the atomic composition of the combined crystalline phases is calculated to be $Si_{20.6}AlO_{2.2}N_{24.2}$. The global atomic composition of this sample (from EPMA) is $Si_{28}Al_5O_{33}N_{32}F_2$, whence, by subtraction, the atomic constitution of the glass is $Si_{7.4}Al_4O_{30.8}N_{1.2}F_2$. The differences in the glass compositions calculated by the two different methods are not surprising in view of the uncertainties in the EPMA analytical method, especially as applied to powders, and the use of simplifying assumptions. These procedures, however, suggest possible approaches to a difficult analytical problem and the results may be regarded as reasonable approximations to the composition of the glass phase in this particular sample.

3.4. *Mechanical and chemical properties*

Table 3 shows the Vickers Hardness values of the β-, O-, and Y-α/β-SiAlON ceramics containing F. These lie in the range 10–12 GPa, lower than literature values of F-free SiAlON (15–17 GPa). The decreased hardness is attributed to the large volume of F-containing glassy phase.

The corrosion of F-containing and F-free single phase β-SiAlON ceramics was carried out at 1300°C in flowing nitrogen containing a constant concentration of NaCl vapor. X-ray diffraction detected only a small amount of mullite on corroded surface of the F-containing SiAlON ceramics. In cross-section, the SEM shows the corroded layer to be compact and less than 10 µm thick [Fig. 6(A)]. Elemental analysis indicated the presence of Al, Si, O, and F but no Na. The absence of Na in the corroded layer suggests that the F-containing SiAlON ceramic is quite resistant to corrosion by NaCl vapor. The presence of Al, Si, and O in the scales indicated the formation of mullite and probably amorphous silica,[19] which may result from oxidation of the SiAlON by the H_2O impurity occurring at a concentration of several ppm in the N_2 gas.

Fig. 6(B) shows the cross-section of the corroded F-free β-SiAlON scale which is seen to be 50 µm thick with 20 µm pores in the central region and several µm sized pores near the interface. The interfacial region also contains a large amount of Na. XRD analysis showed the formation of mullite and α-Al_2O_3 with a large hump at about 25° (2*θ*) indicative of the glassy phase. Needle like crystals 10 µm long and 1–2 µm wide (see arrows) also seen in the scale are Al_2O_3, as indicated by their Al and O content Needle like Al_2O_3 is typically produced

Table 3
Vickers micro-hardness of single phase SiAlON ceramics

Run	SiAlON	GPa
7	O-SiAlON	11.9±1.3
13	β-SiAlON	10.8±3.0
20	β-/Y-α-SiAlON	9.9±0.8

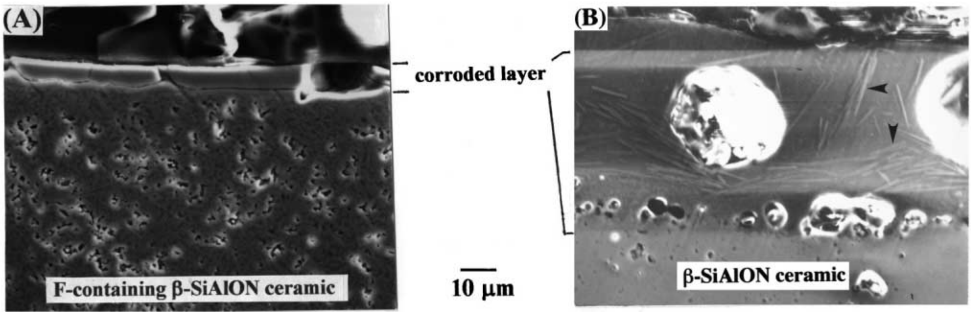

Fig. 6. A cross-sectional SEM image of F-containing and F-free β-SiAlON ceramics exposed to NaCl vapor. (A) F-containing β-SiAlON ceramic, (B) F-free β-SiAlON ceramic. Corrosion conditions: 1300°C for 3 h; flow rate of NaCl vapor 1.0 g h^{-1}.

in sodium silicate melts. It is concluded that the F-containing SiAlON ceramics are strongly resistant to NaCl vapor, in contrast to the F-free SiAlON which was severely corroded by NaCl vapor, with the formation of mullite, sodium silicate and Al_2O_3 crystals.

4. Conclusion

Single phase O-SiAlON ceramic, β-SiAlON ceramic with a trace of mullite and mixture of O-/β- and β-/Y-α-SiAlON ceramics, which all contain F, were synthesized at 1500–1800°C and 150 MPa by HIPing a mixture of Si_3N_4, SiO_2, Al_2O_3, AlN, or Y_2O_3 using AlF_3, or topaz as the source of fluorine. When AlF_3 was used, the single phase F-containing O-SiAlON ceramic ($x = 0.1$) was obtained from a mixture of α-Si_3N_4 and SiO_2 at 1500°C and the mixed O-/β- SiAlONs ceramic at 1700°C. Mixed phase β/Y-α-SiAlONs ceramics were formed from a mixture of α-Si_3N_4, Y_2O_3, and AlN at 1730°C. The use of topaz produced the β-SiAlON ceramic ($z = 0.4$) with a trace of mullite from a mixture of α-Si_3N_4 and AlN at 1770°C and the mixed phases β-/O-SiAlONs ($z = 0.6$ and $x = 0.12$) from a mixture of α-Si_3N_4 and SiO_2 at 1700°C. Single phase of X-SiAlON was not produced in any of the experiments.

The microstructure of the F-containing single phase O-SiAlON ceramic showed it to contain rod-like crystals with a high aspect ratio (30) and platy crystals in a matrix of 30 vol.% glassy phase. In the β-SiAlON ceramic, F-free hexagonal or rod-like crystals with aspect ratios less than 10 were formed in a 20 vol.% glassy phase containing F. The total glass phase was estimated by a quantitative Rietveld XRD powder method. The Y-α/β-SiAlON ceramics contained equiaxed F-free Y-α-SiAlON and hexagonal β-SiAlON crystals in a 10 vol.% glassy matrix containing 25 at.% F.

The Vickers hardness of the F-containing single phase O- and β-SiAlON and β-/Y-α-SiAlON ceramics (10–12 GPa) were lower than literature values for the F-free compounds. The F-containing β-SiAlON ceramics suffered little corrosion in NaCl vapor at 1300°C.

References

1. Riley, F. L., Silicon nitride and related materials. *J. Am. Ceram. Soc.*, 2000, **83**, 245–265.
2. Jack, K. H., Review: sialons and related nitrogen ceramics. *J. Mater. Sci.*, 1976, **11**, 1135–1158.
3. Ekstrom, T. and Nygren, M., SiAlON ceramics. *J. Am. Ceram. Soc.*, 1992, **75**, 259–276.
4. Mitomo, M. and Tajima, Y., Sintering, properties and applications of silicon nitride and sialon ceramics. *J. Ceram. Soc. Jpn.*, 1991, **99**, 1014–1025.
5. Wood, C. A., Zhao, H. and Cheng, Y.-B., Microstructural development of calcium α-SiAlON ceramics with elongated grains. *J. Am. Ceram. Soc.*, 1999, **82**, 421–428.
6. Ekström, T., Jansson, K., Olsson, P-O. and Persson, J., Formation of an Y/Ce-doped α-sialon phase. *J. Eur. Ceram. Soc.*, 1991, **8**, 3–9.
7. Menon, M. and Chen, I.-W., Reaction densification of α-SiAlON: I, wetting behavior and acid-base reactions. *J. Am. Ceram. Soc.*, 1995, **78**, 545–552.
8. Nordberg, L.-O., Nygren, M., Kall, P.-O. and Shen, Z., Stability and oxidation properties of RE-α-SiAlON ceramics (RE = Y, Nd, Sm, Yb). *J. Am. Ceram. Soc.*, 1998, **81**, 1461–1470.
9. Zhan, G.-D., Shi, J.-L., Jiang, D.-Y., Wu, F.-Y., Lai, T.-R. and Yen, T.-S., The effect of crystallization of the grain-boundary phase on ambient temperature fatigue short-crack growth behaviour in Y-α-β-Sialon. *J. Mater. Sci.*, 1996, **31**, 5045–5049.
10. Mandal, H., Camuscu, N. and Thompson, D. P., Comparison of the effectiveness of rare-earth sintering additives on the high-temperature stability of α-sialon ceramics. *J. Mater. Sci.*, 1995, **30**, 5901–5909.
11. Ramesh, R., Byrne, P., Hampshire, S. and Pomeroy, M. J., Kinetics of weight changes and morphological developments during oxidation of pressureless sintered β-SiAlONs. *J. Eur. Ceram. Soc.*, 1997, **17**, 1901–1909.
12. Sheppard, C. M., MacKenzie, K. J. D. and Ryan, M. J., The physical properties of sintered X-phase sialon prepared by Silicothermal reaction bonding. *J. Eur. Ceram. Soc.*, 1998, **18**, 185–191.
13. Ekström, T., Käll, P. O., Nygren, M. and Olsson, P. O., Dense single-phase β-sialon ceramics by glass-encapsulated hot isostatic pressing. *J. Mater. Sci.*, 1989, **24**, 1853–1861.
14. Jun, B.-H., Lee, J.-S., Kim, D.-W., Sung, T.-H., Bae, B.-S. and No, K., Composition, oxidation, and optical properties of fluorinated silicon nitride film by inductively coupled plasma enhanced chemical vapor deposition. *J. Mater. Res.*, 1999, **14**, 995–1001.
15. Kleebe, H.-J., Pezzotti, G. and Nishida, T., Transmission electron microscopy characterization of fluorine-doped Si_3N_4. *J. Mater. Sci. Lett.*, 1995, **14**, 1668–1671.

16. Kleebe, H.-J., Pezzotti, G., Nishida, T. and Rühle, M., Role of interface structure on mechanical properties of fluorine-doped Si_3N_4–SiC ceramics. *J. Ceram. Soc. Jpn.*, 1998, **106**, 17–24.
17. Barris, G., personal communication.
18. Shen, Z. and Nygren, M., On the extension of the α-SiAlON phase area in yttrium and rare-earth doped system. *J. Eur. Ceram. Soc.*, 1997, **17**, 1639–1645.
19. Kiyono, H. and Shimada, S., Kinetics and MAS studies of wet oxidation of β-sialon powders. *J. Electrochem. Soc.* (in press).
20. Day, R. A., Vance, E. R., Cassidy, D. J. and Hartman, J. S., The topaz to mullite transformation on heating. *J. Mater. Res.*, 1995, **10**, 2693.
21. SIROQUANT, Standardless Quantitative XRD Analysis Software, Version 2.0. 1996, Sietronics Pty Ltd.